Photocatalysis of Vaporous Organic Pollutants Using Bead-Shaped Titania Grown on Carbon Fiber†

JOON YEOB LEE and WAN-KUEN JO[*]

Department of Environmental Engineering, Kyungpook National University, Daegu 702-701, Republic of Korea

*Corresponding author: Fax: +82 53 9506579; Tel: +82 53 9506584; E-mail: wkjo@knu.ac.kr

This study was performed to examine the photocatalytic activities of titanium dioxide (TiO_2) grown on carbon fiber sheet (TiO_2-CFS) for purification of air-phase benzene, toluene, ethyl benzene and *o*-xylene (BTEX) under different experimental conditions. The SEM images displayed that TiO_2 could be embedded into the surface of a support CFS by applying a simple hydrothermal technique followed by a calcination process. The XRD results demonstrated that TiO_2 impregnated into CFSs had a photocatalytic function similar to that of TiO_2. The removal efficiencies of BTEX determined *via* the TiO_2-CFSs were all higher than those determined *via* uncalcined CFS. In addition, the removal efficiencies of BTEX determined *via* three TiO_2-CFSs with high amount of TiO_2 imbedded into CFSs were all higher than those determined *via* uncalcined or calcined CFS. Meanwhile, the removal efficiencies of ethyl benzene and *o*-xylene determined *via* the TiO_2-CFS with a low amount of embedded TiO_2 were lower than those determined *via* calcined CFS. As the amount of tetrabutyl titanate used for the preparation of TiO_2-CFSs increased from 2.5 to 6.0 mL, the average removal efficiencies of BTEX increased from 19 to 68 %, 34 to 75 %, 35 to 83 % and 46 to 87 %, respectively. The conditions of high amount of Ti precursor within the range used in the present study, low air flow rates conditions were preferred for decomposition of airborne BTEX. Overall, TiO_2-CFSs could be applied effectively for removal of environmental pollutants, when the amount of Ti precursor was properly chosen for their preparation.

Keywords: Carbon fiber sheet, Hydrothermal process, Calcination.

INTRODUCTION

Vaporous organic pollutants such as benzene, toluene, ethyl benzene and *o*-xylene (BTEX) has received a great deal of attention because of their adverse health effects and prevalence in indoor as well as outdoor air environments. Benzene is a known carcinogen, inducing diseases such as leukemia[1] and other vaporous organic pollutants are highly toxic chemical species causing damage to the nervous system and the liver[2]. These pollutants belong to major monocyclic aromatic hydrocarbons that are often measured in high concentration levels in both urban indoor and outdoor air[3,4]. Typically, both benzene and toluene levels in urban air are higher than those of rural or suburban air[5,6].

Titania (TiO_2) photocatalysis is one of most attractive advanced oxidation techniques, which has proved to be a recent, efficient measure for controlling various environmental contaminants[7-10]. Whereas conventional adsorption method just transfers gas-phase pollutants to another solid phase[11], photocatalysis process has the potential to decompose a wide range

of vaporous organic pollutants to CO_2 and H_2O as a result of oxidation reactions either with hydroxyl radicals and superoxide ions produced after the initial production of highly reactive electron and hole pairs under UV or visible-light irradiation conditions[12,13]. A range of materials have been explored as a photocatalyst supporting material for its environmental pollutant treatment applications. The popularly used supporting materials included activated carbon powders or fibers[14-16], silica gel[17], glass beads[18] and glass tubes[19]. However, the typical substrates-supported photocatalysts were prepared using simple dip coating which has a problem of weak adhesion between supporting substrates and photocatalysts or complicated coating process. To overcome this disadvantage, certain studies[20-22] used carbon fiber sheet (CFS) as a substrate for growing TiO_2 photocatalysts to photocatalytically degrade organic dyes, such as methyl orange, methylene blue and rhodamine B.

Carbon fiber sheet (CFS) is an attractive multipurpose textile that has unique natures over polymer textile. Specifically, CFS is flexible, conductive and stable in high temperature and

corrosive conditions[20,22]. As such, the growth of TiO_2 on CFS (TiO_2-CFS) will still remain a flexible nature but a robust nano-architectural nature. This composite will prevent TiO_2 powders from blowing away with purified air during its air treatment application. In addition, the synergistic effect of carbon and TiO_2 can retard the recombination rates of photogenerated electron and hole pairs, which enhance photocatalytic activity[23,24]. Certain studies[20-22] demonstrated that TiO_2-CFS had superior photocatalytic activity for degradation of aqueous compounds, such as methyl orange, methylene blue and rhodamine B. However, the light absorbance mechanism of photocatalysts and photocatalytic reaction kinetics of environmental pollutants differ at the water-solid and air-solid boundaries[13]. To more accurately determine the photocatalytic activity of such systems, this study examined the photocatalytic activities of TiO_2-CFS for purification of air-phase benzene, toluene, ethyl benzene and *o*-xylene (BTEX) under different experimental conditions. Benzene, toluene, ethyl benzene and *o*-xylene were chosen as target pollutants based on its prevalence in indoor environments and their toxic properties[1,3].

EXPERIMENTAL

Synthesis and characterization of TiO_2-CFS: TiO_2-CFS was synthesized using a simple hydrothermal technique following by a calcination process. 2.4, 3.0, 4.0 or 6.0 mL of tetrabutyl titanate [$Ti(OBu)_4$, TBT, Sigma-Aldrich] was slowly added to 72 mL of hydrochloric acid (HCl 5 M, Merck), after which this mixture was stirred for 0.5 h. Subsequently, this solution was added to 1.2 mL of hydrofluoric acid (HF 47 %, Merck) and then stirred for 5 min. This product (75.6-79.2 mL) was transferred into a Teflon-lined stainless steel autoclave with a capacity of 170 mL and 3.5 g of CFS (8.5 cm × 24.0 cm) was then immersed in this solution. The hydrothermal process was performed at 180 ℃ in an electric oven for 4 h and then cooled to room temperature. Then, the CGS was ultrasonically cleaned for 3 min in a mixture of isopropyl alcohol (200 mL) and distilled water (100 mL), after which this product was treated with NaOH (0.1 M, Merck) to remove fluorine ions adsorbed onto the CFS. The final products were calcined at 350 ℃ in an electric furnace for 1 h to obtain TiO_2-CFSs.

The TiO_2-CFSs prepared using 2.4, 3.0, 4.0 and 6.0 mL of tetrabutyl titanate were designated as TiO_2-CFS-2.4, TiO_2-CFS-3.0, TiO_2-CFS-4.0 and TiO_2-CFS-6.0, respectively. These photocatalysts, along with uncalcined and calcined CFSs, were characterized using field emission scanning electron microscopy (FE-SEM, Hitachi S-4300 & EDX-350) and X-ray diffraction (XRD, Rigaku D/max-2500). The surface morphological images were observed by FE-SEM at an acceleration voltage of 15 kV. The XRD images were determined using CuK_α radiation operated at 40 kV and 100 mA in the range of 20-80° (2θ-θ) at a scanning rate of 3° min^{-1}.

Photocatalytic performance tests: The photocatalytic performance of the as-prepared TiO_2-CFSs for decomposition of gaseous BTEX were investigated under UV irradiation. For comparison, the removal efficiencies of BTEX *via* uncalcined and calcined CFSs were also determined under a fixed condition. The photocatalytic activity tests were performed using a continuous-flow Pyrex reactor with 4.3 cm i.d. and 26.5 cm

length, whose inner wall was covered with a TiO_2-CFS, uncalcined, or calcined CFS. A cylindrical UV source (8-W fluorescent black light lamp, F8T5BLB, Youngwha Lamp Co.) was inserted inside the photocatalytic reactor and acted as the inside surface boundary layer of the cylindrical reactor. A standard gas was prepared by mixing humidified air with the target compounds injected into a buffering chamber *via* an auto-programmed syringe pump (Model Legato 100, KdScientific Inc.). The standard gas stream flowed into an empty buffering chamber to minimize the inlet concentration fluctuation and fed into the reactor. The air flow rates (AFR) and the relative humidity (RH) were measured using mass flow controllers (Defender 510, Bios International Co.) and a humidity meter (TR-72S, T & D Co.), respectively. The experimental conditions varied on the basis of AFRs, input concentrations (ICs) and relative humidity. The AFR range for these experiments was set at 1.0-4.0 L/min (1.0, 2.0, 3.0 and 4.0 L min^{-1}), covering a broad flow range. The IC and RH were fixed to 0.1 ppm and 45 %, respectively. Gaseous chemicals in the air stream were measured at the upstream and downstream ports of the Pyrex reactor. Gas samples were collected by filling an evacuated 5 L Tedlar bag and then, air from this bag was drawn through a stainless steel adsorbent trap. The gaseous species adsorbed on the trap were analyzed using an automatic thermal desorber (ATD 400, Perkin Elmer Co.) coupled to a gas chromatograph (GC, 7890, Agilent Inc.) with a flame ionization detector (FID) and a capillary column (DB-1, Agilent Co.).

RESULTS AND DISCUSSION

Morphological properties of TiO_2-CFS, uncalcined and calcined CFSs: The particle morphologies of TiO_2-CFSs, uncalcined and calcined CFSs were examined using SEM and XRD patterns. Fig. 1 shows the SEM images of TiO_2-CFS-2.4, TiO_2-CFS-3.0, TiO_2-CFS-4.0 and TiO_2-CFS-6.0, uncalcined and calcined CFSs. As shown in previous studies[20-22], TiO_2 photocatalysts could be embedded into the surface of a support material (CF) by applying the described preparation method. The calcined CFS displayed a fiber shape similar to that of uncalcined CFS. The TiO_2 embedded into the CFSs exhibited bead shapes and as expected, the amounts of embedded TiO_2 increased as the amounts of TBT used for the preparation of TiO_2-CFSs increased. In particular, the TiO_2-CFS-2.4 exhibited many uncovered or partially-covered CFSs, indicating lower photocatalytic activity of this photocatalyst relative to other TiO_2-CFSs. The space between adjacent CFSs appeared to be sufficient to allow the penetration of light into the fibrous photocatalysts to a certain depth.

Fig. 2 showed the XRD images of TiO_2-CFS-6.0, uncalcined and calcined CFSs. Similar noise peaks were noted for the calcined and uncalcined CFSs. However, the TiO_2-CFS-6.0 revealed an anatase crystal phase with a distinct peak at 2θ = 25.2° and a rutile crystal phase with a distinct peak at 2θ = 27.4°, whereas the uncovered CFSs did not any crystal phase peaks. These results demonstrated that TiO_2 impregnated into CFSs had a photocatalytic function similar to that of TiO_2, which was consistent with that obtained using another TiO_2-CFS system[20]. Additionally, a broad shallow peak located at 2θ = 44° for both the uncovered and TiO_2-CFSs composite
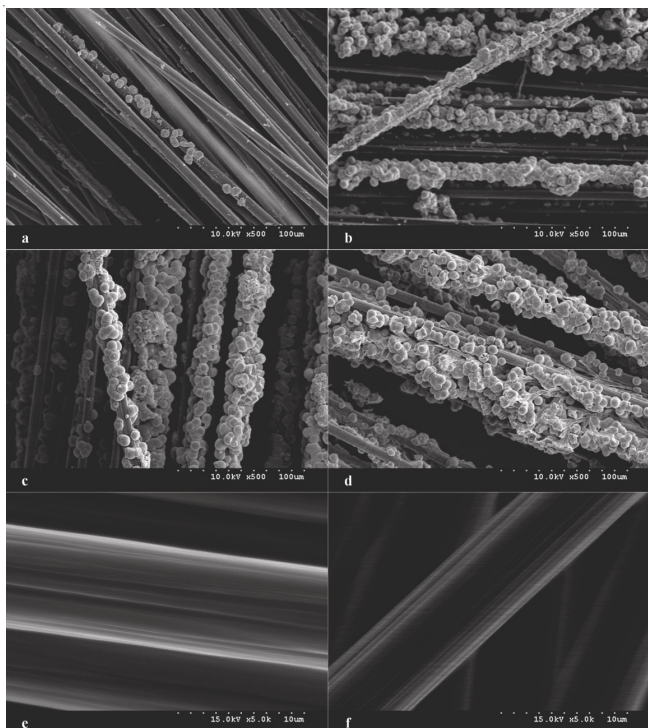
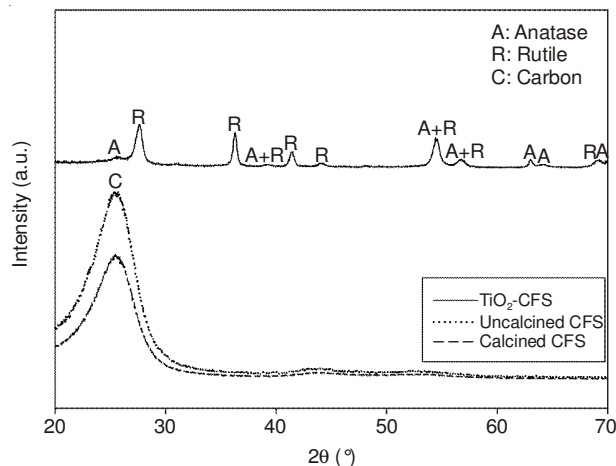Fig. 1.　Scanning electron microscopy of TiO₂-CFS-2.4, TiO₂-CFS-3.0, TiO₂-CFS-4.0, and TiO₂-CFS-6.0, uncalcined and calcined CFSs

Fig. 2.　X-Ray diffraction pattern of TiO₂-CFS-6.0, uncalcined and calcined CFSs

was ascribed to carbon, which would reflect the presence of CFS[20].

Removal of BTEX *via* TiO₂-CFSs, uncalcined and calcined CFSs: The removal efficiencies of BTEX *via* TiO₂-CFSs, uncalcined and calcined CFSs were investigated under different experimental conditions. Fig. 3 displays the time-series removal efficiency of BTEX as determined *via* TiO₂-
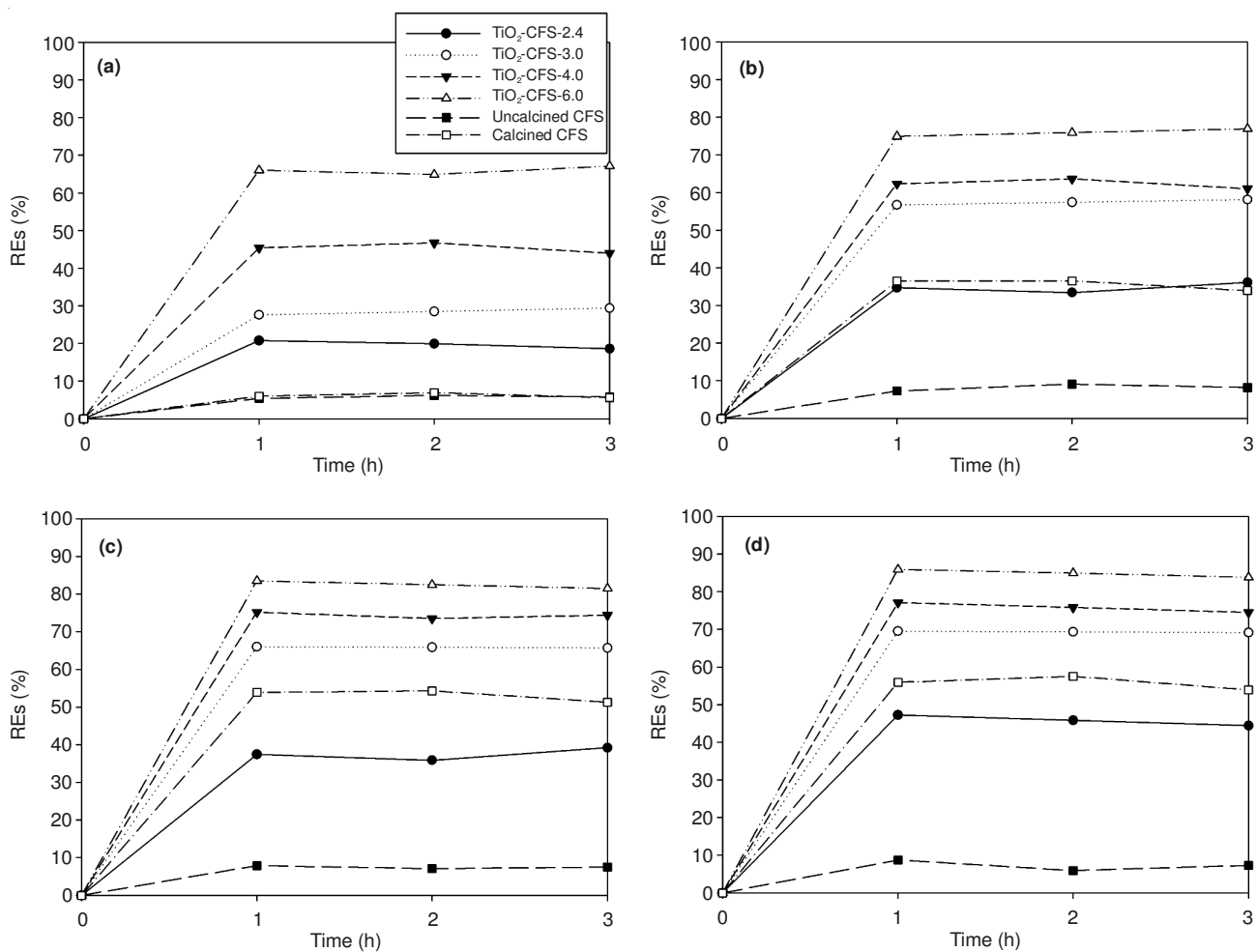

Fig. 3.　Removal efficiencies (REs, %) of (a) benzene, (b) toluene, (c) ethyl benzene, and (d) *o*-xylene as determined *via* TiO₂-CFS-2.4, TiO₂-CFS-3.0, TiO₂-CFS-4.0, and TiO₂-CFS-6.0, uncalcined and calcined CFSs under UV irradiation

CFS-2.4, TiO$_2$-CFS-3.0, TiO$_2$-CFS-4.0 and TiO$_2$-CFS-6.0, uncalcined and calcined CFSs under UV irradiation. The removal efficiencies of BTEX determined *via* the TiO$_2$-CFSs were all higher than those determined *via* uncalcined CFS. In addition, the removal efficiencies of BTEX determined *via* three TiO$_2$-CFSs with high amount of TiO$_2$ imbedded into CFSs (TiO$_2$-CFS-3.0, TiO$_2$-CFS-4.0 and TiO$_2$-CFS-6.0) were all higher than those determined *via* uncalcined CFS, although the removal efficiencies of ethyl benzene and *o*-xylene determined *via* the TiO$_2$-CFS-2.4 were lower than those determined *via* calcined CFS. Similarly, for removal of aqueous-phase rhodamine-B, Chen *et al.*[20] reported that the photocatalytic activity of TiO$_2$ nanotube arrays formed on CFSs for removal of aqueous-phase rhodamine B was higher than those of untreated CFSs. These resuts suggested that, regradless of the phases, TiO$_2$-CFSs could be applied effectively for removal of environmental pollutants. The removal efficiencies of BTEX increased as the amount of Ti precursor (TBT) increased, indicating that the amount of Ti precursor was an important factor for the removal mechanism of the TiO$_2$-CFS photocatalytic system.

The time-series removal efficiencies of BTEX as determined *via* TiO$_2$-CFS-6.0 according to AFR are shown in Fig. 4. The removal efficiencies of BTEX decreased with increasing AFRs, which was similar to other photocatalytic studies[25,26]. As the air flow rates was increased from 1.0 to 4.0 L min^{-1}, the average removal efficiencies of BTEX decreased from 68 to 32 %, 75 to 52 %, 83 to 53 % and 87 to 68 %, respectively, indicating that AFR was still an influential factor for the removal mechanism of the TiO$_2$-CFS photocatalytic system. As AFR increased, the bulk mass transport of BTEX molecules from the air-phase to the catalyst surface that is a key photo-catalytic reaction process would increase primarily due to convection and diffusion phenomena. As such, the oxidation rate would increase as AFR increased, indicating that the decomposition of BTEX was limited to the photocatalyst surface reaction. However, this trend was not consistent with that obtained from the present study. At higher AFR the gas retention time in the photocatalytic reactor would be too short to provide sufficient BTEX transfer from the air phase to the solid catalyst surface[25]. Consequently, decreased efficiencies at higher AFRs indicate that an insufficient reactor retention time effect would exceed the bulk mass transport effect on decomposition of BTEX molecules on the catalyst surfaces.

Conclusion

The present study examined the applicability of TiO$_2$-CFSs for the photocatalytic decomposition of gas-phase BTEX under
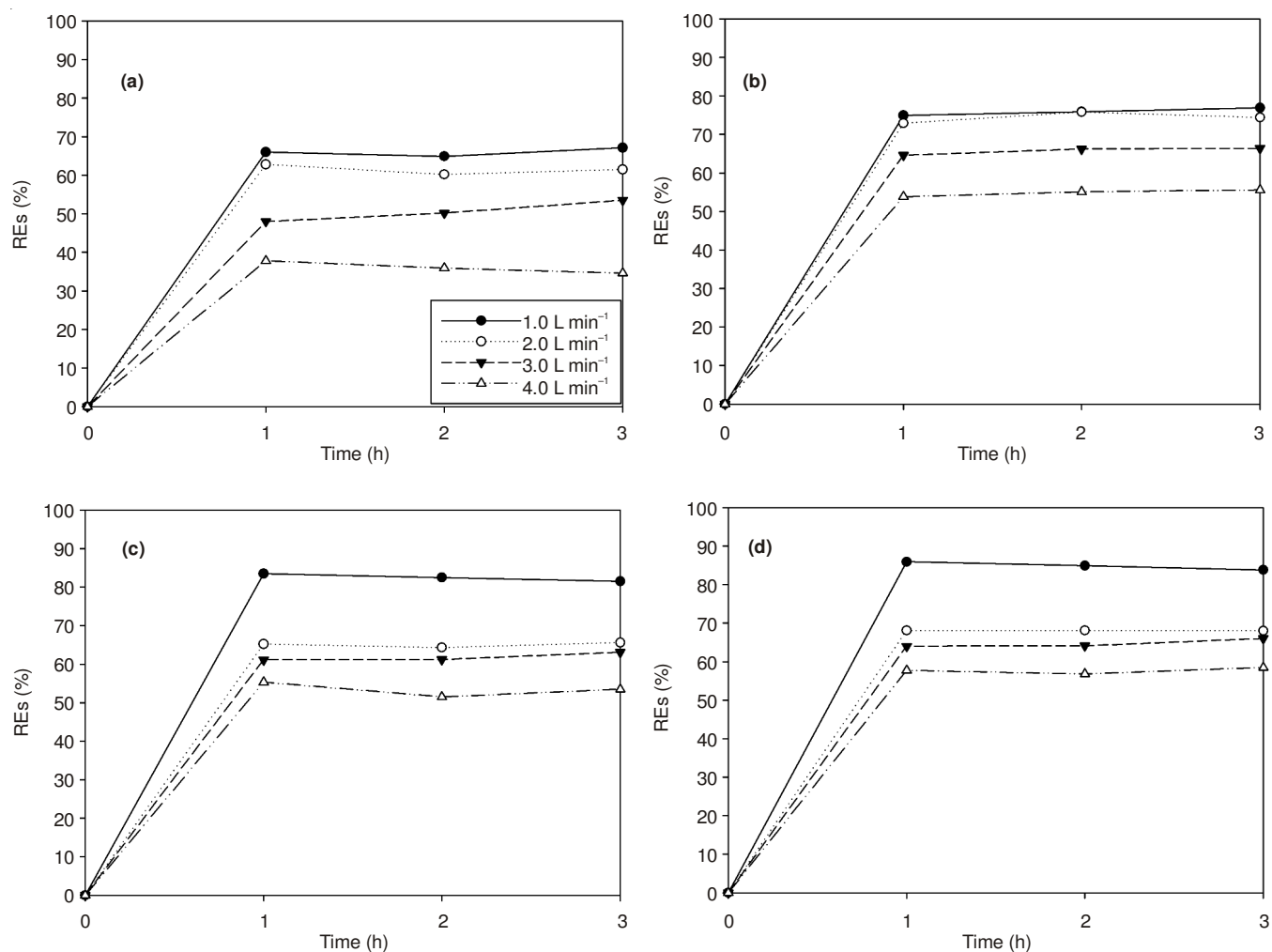

Fig. 4.   Removal efficiencies (REs, %) of (a) benzene, (b) toluene, (c) ethyl benzene and (d) *o*-xylene as determined *via* TiO$_2$-CFS-6.0 according to air flow rates (1.0, 2.0, 3.0, and 4.0 L min^{-1})

a range of experimental conditions. The SEM results demonstrated that TiO_2 photocatalysts could be embedded into the surface of a support material (CF) by applying the described preparation method. The XRD patterns showed that TiO_2 impregnated into CFSs had a photocatalytic function similar to that of TiO_2. Another major finding was that TiO_2-CFSs could be applied effectively for removal of environmental pollutants, when the amount of Ti precursor was properly chosen for their preparation. In addition, the conditions of high amount of Ti precursor within the range used in the present study, low AFR conditions were preferred for decomposition of airborne BTEX.

ACKNOWLEDGEMENTS

REFERENCES

1. IARC (International Agency for Research on Cancer), Monographs on the evaluation of the carcinogenic risks of chemicals to man, WHO, Geneva (2004).
2. A.S. Revilla, C.R. Pestana, G.L. Pardo-Andreu, A.C. Santos, S.A. Uyemura, M.E. Gonzales and C. Curti, *Toxicol. in Vitro*, **21**, 782 (2007).
3. T. Ohura, T. Amagai, X. Shen, S. Li, P. Zhang and L. Zhu, *Atmos. Environ.*, **43**, 6352 (2009).
4. U. Schlink, A. Thiem, T. Kohajda, M. Richter and K. Strebel, *Sci. Total Environ.*, **408**, 3840 (2010).
5. C. Jia, S. Batterman and C. Godwin, *Atmos. Environ.*, **42**, 2101 (2008).
6. D. Pérez-Rial, P. López-Mahía and R. Tauler, *Atmos. Environ.*, **44**, 5122 (2010).
7. H. Choi, E. Stathatos and D.D. Dionysiou, *Desalination*, **202**, 199 (2007).
8. C. Bougheloum and A. Messalhi, *Phys. Proc.*, **2**, 1055 (2009).
9. A.H. Aïssa, E. Puzenat, A. Plassais, J.-M. Herrmann, C. Haehnel and C. Guillard, *Appl. Catal. B*, **107**, 1 (2011).
10. W.K. Jo and H.J. Kang, *Appl. Surf. Sci.*, **259**, 657 (2012).
11. C.-Y. Lu and M.-Y. Wey, *Fuel Process. Technol.*, **88**, 557 (2007).
12. V. Augugliaro, M. Litter, L. Palmisano and J. Soria, *J. Photochem. Photobiol. Chem.*, **7**, 127 (2006).
13. M.A. Henderson, *Surf. Sci. Rep.*, **66**, 185 (2011).
14. C.H. Ao and S.C. Lee, *Chem. Eng. Sci.*, **60**, 103 (2005).
15. J. Matos, E. García-López, L. Palmisano, A. García and G. Marcì, *Appl. Catal. B*, **99**, 170 (2010).
16. W.K. Jo, S.H. Shin and E.S. Hwang, *J. Hazard. Mater.*, **191**, 234 (2011).
17. H. Yamashita, S. Nishio, I. Katayama, N. Nishiyama and H. Fujii, *Catal. Today*, **111**, 254 (2006).
18. S.W. Verbruggen, S. Ribbens, T. Tytgat, B. Hauchecorne, M. Smits, V. Meynen, P. Cool, J.A. Martens and S. Lenaerts, *Chem. Eng. J.*, **174**, 318 (2011).
19. H.H. Chun and W.K. Jo, *Chin. J. Catal.*, **34**, 1256 (2013).
20. P. Chen, L. Gu, X. Xue, M. Li and X. Cao, *Chem. Commun.*, **46**, 5906 (2010).
21. N.K. Dey, M.J. Kim, K.-D. Kim, H.O. Seo, D. Kim, Y.D. Kim, D.C. Lim and K.H. Lee, *J. Mol. Catal. A*, **337**, 33 (2011).
22. W. Guo, F. Zhang, C. Lin and Z.L. Wang, *Adv. Mater.*, **24**, 4761 (2012).
23. B. Jiang, C. Tian, Q. Pan, Z. Jiang, J.-Q. Wang, W. Yan and H. Fu, *J. Phys. Chem. C*, **115**, 23718 (2011).
24. R. Leary and A. Westwood, *Carbon*, **49**, 741 (2011).
25. J. Jeong, K. Sekiguchi, W. Lee and K. Sakamoto, *J. Photochem. Photobiol. A*, **169**, 279 (2005).
26. Q.L. Yu and H.J.H. Brouwers, *Appl. Catal. B*, **92**, 454 (2009).